Geobiology (2006), **4**, 123–136

Microbial fuel cell energy from an ocean cold seep

C. E. REIMERS,[1] P. GIRGUIS,[2,3] H. A. STECHER III,[1] L. M. TENDER,[4] N. RYCKELYNCK[1] AND P. WHALING[2]

[1]*Hatfield Marine Science Center and College of Oceanic and Atmospheric Sciences, Oregon State University, Newport, Oregon, USA*
[2]*Monterey Bay Aquarium Research Institute, Moss Landing, California, USA*
[3]*Biological Laboratories, Harvard University, Cambridge, Massachusetts, USA*
[4]*Naval Research Laboratory, Center for Bio/Molecular Science and Engineering, Washington DC, USA*

ABSTRACT

Benthic microbial fuel cells are devices that generate modest levels of electrical power in seafloor environments by a mechanism analogous to the coupled biogeochemical reactions that transfer electrons from organic carbon through redox intermediates to oxygen. Two benthic microbial fuel cells were deployed at a deep-ocean cold seep within Monterey Canyon, California, and were monitored for 125 days. Their anodes consisted of single graphite rods that were placed within microbial mat patches of the seep, while the cathodes consisted of carbon-fibre/titanium wire brushes attached to graphite plates suspended ~0.5 m above the sediment. Power records demonstrated a maximal sustained power density of 34 mW·m^{-2} of anode surface area, equating to 1100 mW m^{-2} of seafloor. Molecular phylogenetic analyses of microbial biofilms that formed on the electrode surfaces revealed changes in microbial community composition along the anode as a function of sediment depth and surrounding geochemistry. Near the sediment surface (20–29 cm depth), the anodic biofilm was dominated by micro-organisms closely related to *Desulfuromonas acetoxidans*. At horizons 46–55 and 70–76 cm below the sediment–water interface, clone libraries showed more diverse populations, with increasing representation of δ-proteobacteria such as *Desulfocapsa* and *Syntrophus*, as well as ε-proteobacteria. Genes from phylotypes related to *Pseudomonas* dominated the cathode clone library. These results confound ascribing a single electron transport role performed by only a few members of the microbial community to explain energy harvesting from marine sediments. In addition, the microbial fuel cells exhibited slowly decreasing current attributable to a combination of anode passivation and sulfide mass transport limitation. Electron micrographs of fuel cell anodes and laboratory experiments confirmed that sulfide oxidation products can build up on anode surfaces and impede electron transfer. Thus, while cold seeps have the potential to provide more power than neighbouring ocean sediments, the limits of mass transport as well as the proclivity for passivation must be considered when developing new benthic microbial fuel cell designs to meet specific power requirements.

Received 17 November 2005; accepted 09 February 2006

Corresponding author: C. E. Reimers. Tel.: 541-867-0220; fax: 541-867-0138; e-mail: creimers@coas.oregonstate.edu.

INTRODUCTION

Microbial fuel cells are tangible proof that bacteria use organic substrates to produce reducing power and to transfer electrons through exogenous materials to oxidants in the environment (Bennetto *et al.*, 1983; Schröder *et al.*, 2003; Ieropoulos *et al.*, 2005). However, many unanswered questions remain about the basic charge transfer mechanisms of these systems, their time- and environment-dependent behaviour, the roles of different micro-organisms and substrates in electricity production, and how to enhance, balance and maintain electrode reactions to increase power and optimize energy recovery (He *et al.*, 2005; Liu *et al.*, 2005).

The benthic microbial fuel cell (BMFC) is a field-deployable and uniquely configured microbial fuel cell that relies on the natural redox processes in aqueous sediments. These fuel cells are under development as long-term power sources for autonomous sensors and acoustic communication devices deployed in fresh and salt water environments (Reimers *et al.*, 2001; Tender *et al.*, 2002; Holmes *et al.*, 2004b; Alberte *et al.*, 2005). We consider the BMFC mechanism as being analogous to the coupled microbial and chemical reactions yielding

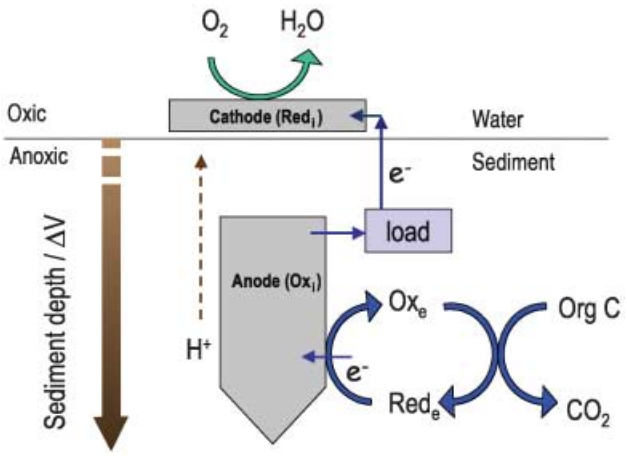

Fig. 1 A schematic diagram of the BMFC. If the electrodes of a BMFC are not electrically connected (i.e. open circuit condition), their voltages equilibrate to the redox potentials of their respective environments. However, if BMFC electrodes are electrically connected through a resistive load, electrons will flow from the more negative anode to the cathode, which reduces the whole cell voltage and raises the potential at the anode. When the anode potential is raised, it starts to simulate an intermediate electron acceptor (Ox_i) and the cathode then acts as an intermediate donor (Red_i) between environmental reductants (Red_e, that may be organic or inorganic products of anaerobic metabolism) and dissolved oxygen. Micro-organisms may facilitate many of the illustrated electron transfers, and these transfers may occur inside a biofilm or at the biofilm–solution interface.

energy and carrying electrons from organic carbon to oxygen in natural sediments (Aller, 1994; Burdige, in press) (Fig. 1). The essential components of the BMFC are a pair of non-corrosive (e.g. graphite) electrodes electrically connected through an external circuit and positioned such that one electrode (anode) is imbedded in anoxic sediment and the other electrode (cathode) is in overlying oxic water. The biologically active sediment surface layer separates natural reductants and oxidants, and it enables counter ion flow (e.g. H^+) between the electrodes of the BMFC. Microbial biofilms that form naturally on the electrode surfaces have a contentious and poorly documented role in electron transfer except in simple monoculture laboratory MFCs. It may be that natural biofilms contain micro-organisms that use electrodes directly as electron acceptors or donors (Bond *et al.*, 2002; Bond & Lovley, 2003; Holmes *et al.*, 2004a; Reguera *et al.*, 2005), or it may be that electron transfer occurs indirectly through extracellular electron shuttles which can be either exogenous or endogenous, and inorganic or organic (Rabaey *et al.*, 2004; Ieropoulos *et al.*, 2005).

The present article addresses new information about the electrode biofilm communities and other physical and chemical processes that can impact the delivery of current in the complex biogeochemical environment surrounding a BMFC. Since BMFCs require anoxic sediments overlain by oxic waters, the areas of the ocean most suited for their application are found on continental margins. In these settings, organic carbon fluxes from surface waters generally exceed 4 g C m^{-2} y^{-1} (Muller-Karger *et al.*, 2005), and it is not unusual to also find locations where organic substrates and reductants are supplied from the subsurface by geological forces. We report the results of an environmental pilot-scale experiment in which two identical BMFCs were tested at a marine 'cold seep' for over four months. The sulfide- and methane-rich fluids that fuel chemosynthetic biological communities at seeps were hypothesized to be ideal for supporting higher power production by BMFCs. We wished to determine if microbial communities unique to seeps might aid electron transfer directly (vis-à-vis Reguera *et al.*, 2005) or else have indirect interactions, for example with sulfur deposits that modify electrode surfaces. Such interactive behaviour was indicated by the geochemical impacts and microbial analyses of earlier demonstration experiments of BMFCs within estuarine and salt-marsh environments (Tender *et al.*, 2002; Ryckelynck *et al.*, 2005). Laboratory fuel cell experiments were also designed to uncouple biological factors from electrochemical sulfide oxidation, anodic passivation and mass transport variations to better understand aspects of BMFC performance.

ENVIRONMENTAL SETTING

The seepage sites studied were aligned approximately 5 m apart along a slope known as Extravert Cliff, 36°46′30″N, 122°05′10″W, located at 957 m water depth in Monterey Bay, California. Fluids that migrate through permeable horizons to the seafloor in this area originate due to subsurface compression and strike-slip faulting, or by a form of slow mud diapirism (Embley *et al.*, 1990; Orange *et al.*, 1999). On continental margins worldwide, similar sites are often related to subsurface methane gas hydrates (Borowski *et al.*, 1999; Tryon *et al.*, 2002). Seafloor patches capped with mats of sulfide-oxidizing bacteria and surrounded by dense aggregations of vesicomyid clams were used to target fuel cell placement (Fig. 2A, Barry *et al.*, 1997; Rathburn *et al.*, 2003).

EXPERIMENTAL

Pore water studies

Two years prior to this energy harvesting study, pore water chemical distributions were measured within Extravert Cliff sediments to depths of 120 cm using 'vibrapeepers' (Plant *et al.*, 2001). The lance-like 'vibrapeeper' has two columns of membrane-covered 5 cm^3 wells on parallel polycarbonate faces and is designed to equilibrate with surrounding solutions after being vibrated into the sediment to depths of 130 cm. Two vibrapeepers (VP1 and VP2) were deployed at positions within seep rings and one (VP3) approximately 5 m outside these rings from June 5 to July 11 2001. Concentrations of total sulfide (ΣS^{-2}) in pore waters were determined immediately after retrieval according to Cline (1969), and

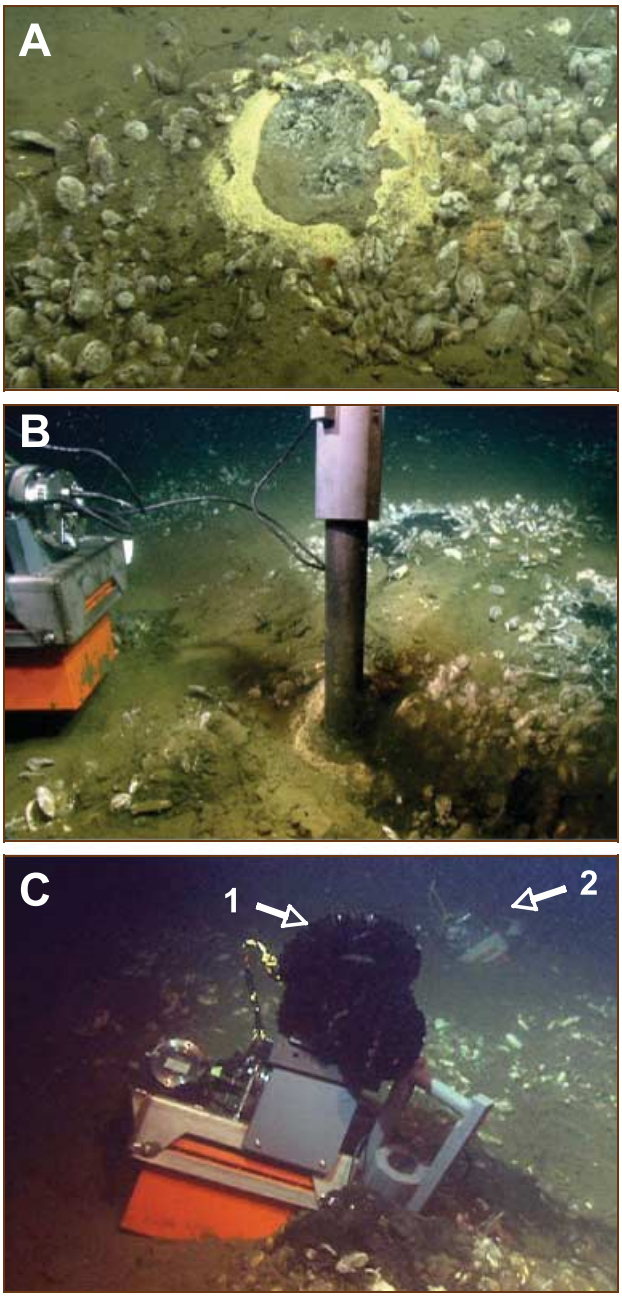

Fig. 2 (A) Seep ring at Extravert Cliff where FC1 was placed. (B) FC1 anode being inserted by the ROV *Ventana*. (C) FC2 showing cathode carbon-brushes (1 arrow) and graphite plate mounted to a PVC plate above the load housing and battery. The anode is buried to the right so that only the PVC cap and handle are visible. FC1 is in the background (2 arrow).

sulfate and chloride were determined subsequently by anion chromatography and by titration with $AgNO_3$ to an electrochemical endpoint, respectively. The sample splits saved for ion chromatography were first purged of sulfide by acidification and bubbling with nitrogen gas.

During the timeframe of this study, near surface pore water distributions were determined anew. Acrylic tubes (7.6 cm i.d. × 35 cm long) configured as 'push-corers' were used to collect sediment cores in the vicinity of the fuel cells soon after their installation. Four of these cores were later processed under a N_2 atmosphere at 4 °C to retrieve pore waters from 0.5 to 4 cm thick depth sections for chemical characterization as described above.

Benthic microbial fuel cells

The patchiness of the Extravert Cliff seeps and the concentration profiles of pore fluids determined by Plant *et al.* (2001) were used as guiding factors for anode design. Accordingly, two anodes (one for each BMFC) were fabricated from 8.4-cm diameter × 91.4-cm graphite rods (Grade G-10, Graphite Engineering and Sales, Greenville, MI, USA). The bottom 15.2 cm of each graphite rod was tapered to a point, while the top 15.2 cm of the rod was turned down to 7-cm diameter to fit within a PVC sleeve (30.1 cm long, 12.7 cm OD). A two-conductor, 20 ga waterproof cable (IE2F-5/8 Impulse Enterprises, San Diego, CA, USA) was terminated with an underwater-pluggable connector and attached to the top centre of the rod using a titanium bolt and conductive epoxy (TIGA Silver 901). Finally, the anode was inserted into the PVC sleeve and the wire connection potted by partially filling the void space with marine-grade epoxy (West System 205/207). The resulting outer surface area of exposed graphite for each anode was thus 0.184 m^2, while the area of seafloor occupied (footprint) was only 0.0057 m^2.

Each cathode was constructed from a graphite plate (Grade G-10; 25.4 × 12.7 × 1.3 cm; Graphite Engineering) to which a waterproof electrical cable and two 1-m long 'carbon-brush' electrodes (consisting of fine carbon fibers in high density on titanium wires, Hasvold *et al.*, 1997) were attached using titanium bolts. Two reference electrodes, fabricated from bare silver wires (1.27 mm diameter) plated with AgCl, completed each system. At bottom-water chloride concentrations of 538 mmol kg^{-1} and bottom-water temperatures of 4 °C, the potentials of these reference electrodes are predicted to be 236 mV vs. SHE according to the Nernst equation (Brett & Brett, 2002).

The fuel cell and reference electrodes were connected to a passive preprogrammed load and data logger (Model 871; Scribner Associates, Southern Pines, NC, USA) contained in a stainless steel housing equipped with bulkhead underwater-pluggable connectors. Power for the load and data logger was supplied by a 12-V deep-ocean lead-acid battery (Deep Sea Power and Light, San Diego, CA, USA). The load, cathode and battery were bolted onto a stainless steel and PVC frame that served to raise the cathode well above the sediments (Fig. 2C).

On May 21 and 23, 2003, the two BMFCs (FC1 and 2) were placed using the remotely operated vehicle (ROV) *Ventana* within seep rings at Extravert Cliff (Fig. 2). During each deployment, an anode was centred over patches of bacterial

mat with the ROV manipulator arm, then its entire length was pushed into the seafloor leaving only the PVC handle exposed (Fig. 2C). Each cathode and monitoring load package was positioned within 0.5 m from its respective anode. The experimental programs, designed to control whole-cell voltage (cathode vs. anode) using two-electrode amperometry (Bard & Faulkner, 2001) while logging whole-cell potential, anode potential (anode vs. reference) and current once an hour for 125 days, were initiated on shipboard immediately before the start of each deployment. These programs included periods when the cell voltage was reduced daily to fixed values in progressive steps (a form of polarization testing; days 20–31 and 103–114) as well as longer periods of discharge at either 0.6 or 0.3 V. After day 125 when data logging ceased, whole-cell potentials continued to be maintained at 0.3 V.

Electrode recoveries, sampling and analyses

Both fuel cells were removed from the seafloor during separate ROV *Ventana* dives on October 7, 2003. Unfortunately the anode from FC1 was lost from the ROV sled on its trip to the surface, so could not be sampled. Microbiological sampling of the remaining anode and the two cathodes was started immediately after their recoveries to the surface vessel. The graphite rod of the FC2 anode was thoroughly rinsed with a 0.2-μm filter-sterilized 1 : 1 solution of ethanol and isoosmotic phosphate-buffered saline (EtOH/PBS) to remove any visible debris or sediment. Three regions of the anode, located between 5 and 14 cm, 30 and 39 cm and 56 and 62 cm from the top of the exposed length of graphite (hereafter, TOP, MIDDLE and BOTTOM, respectively), were scraped with a sterile razor blade (to gather microbial biomass), and then the scrapings were transferred to scintillation vials. Video records indicated these samples were in contact with sediment approximately 20–29, 46–55 and 70–76 cm below the sediment–water interface. Two milliliters of sterile lysis buffer (containing 0.73 M sucrose, 50 mM Tris buffer adjusted to pH 8.3, 40 mM EDTA, and 50 mg lysozyme per mL of buffer) was added to each sample and thoroughly mixed. Similarly, bundles of carbon fibers were clipped with sterile surgical scissors from the cathodes, transferred to sterile glass scintillation vials and filled with 2 mL of lysis buffer as described above. All samples were frozen at −80° within 2 h of sampling and remained frozen until later extraction procedures.

A second set of electrode samples were collected for electron microprobe surface analyses. Wedge-shaped samples of graphite (2–3 cm long by 0.5 cm deep, with one face perpendicular to the external surface) were cut from the FC2 anode with a Dremel tool within an hour after recovery on board ship. The areas sampled were located between 8 and 14, 26–30 and 49–52 cm from the upper end of the exposed anode with four to five samples per area (TOP, MIDDLE, BOTTOM for microprobe). After rinsing with sterile seawater, each piece was embedded in hydrophilic epoxy (Nanoplast FB-101 embedding resin kits, SPI supplies, West Chester, PA, USA). These embedded samples were later trimmed and embedded a second time using molds to form 2.5 cm diameter discs. The cross-sectional face of the graphite was orientated up. Sample polishing was carried out with progressively finer grades of abrasive. Electron microprobe analyses were performed along preprogrammed transects with an accelerating potential of 15.1 kV, a beam current of 49.0 nA, and a beam size of 5 μm. Scanning electron microscope backscatter images and elemental X-ray maps for S, Fe, Si, and O were recorded in association with the microprobe measurements.

Bottom-water properties

During both deployment and recovery ROV dives to the study site, bottom-water properties were measured with a CTD equipped with an added O_2 sensor (Falmouth Scientific, Cataumet, MA, USA). Water samples were also collected approximately 1 m above bottom in Niskin bottles tripped by the ROV during the deployment dives. These water samples were subsampled and fixed with Winkler reagents for later determinations of dissolved O_2 (Knapp *et al.*, 1990) as checks on the sensor data. Water subsamples from the Niskins were also frozen for later determinations of dissolved nutrients.

Nucleic acid purification and extraction

Prior to extraction, all microbiological samples were thawed to room temperature and the graphite fibers or scrapings were transferred to preweighed 2 mL screw-top cryovials containing 1 g of zirconium beads and approximately 0.5 mL of sterile lysis buffer. Each tube was tared and weighed on an electronic balance (Mettler-Toledo Inc., Columbus, OH, USA) to determine the mass of the graphite. Nucleic acids were extracted using the PowerSoil DNA extraction kit (MoBio Inc., San Diego, CA, USA) modified to maximize yields as described in Girguis *et al.* (2003). This procedure produced DNA fragments between 10 and 25 kb in size.

Bacterial small subunit rRNA library construction

Small subunit (SSU) rRNA bacterial genes from all samples were amplified by polymerase chain reaction (PCR). Each 50 μL PCR contained 0.2 μM of a bacterial-targeted forward primer (B27f, 59-AGAGTTTGATCCTGGCTCAG-39) and a universal reverse primer (U1492r, 59-GGTTACCTTGTTACGACTT-39), 5 μL of PCR buffer (containing 2 mM $MgCl_2$; Invitrogen Inc.), 2.5 mM each deoxynucleotide triphosphate, and 0.025 U of *Taq* polymerase (Platinum TAQ; Invitrogen Inc., Carlsbad, CA, USA). DNA was amplified for 25 cycles with an initial denaturation and heat activation step of 2 min at 95 °C, and 25 cycles of 30 s at 94 °C, 30 s at 55 °C, and 45 s at 72 °C. A final 7-min extension at 72 °C was

added to facilitate A-tailing and subsequent cloning of amplified products. To construct environmental rRNA clone libraries, amplicons were pooled from three reactions and concentrated in Microcon YM-100 (Millipore Inc., Billerica, MA, USA) spin filters. Amplicons were cloned into a pCR4 TOPO vector, and transformed into chemically competent *Escherichia coli* according to the manufacturer's protocol (TOPO TA cloning kit, Invitrogen Inc.). Transformants were screened on LB-kanamycin-XGAL plates using blue-white selection. Colonies were grown in 2× LB media-kanamycin for 48 h. Plasmids were then purified using the Montage miniprep kit (Millipore, Inc.), and sequenced with BigDye chemistry (version 3.1) on an ABI 3100 capillary sequencer (Applied Biosystems Inc., Foster City, CA, USA). Between 192 and 384 clones from each sample were sequenced in both directions.

Phylogenetic analysis

SSU rRNA sequences were trimmed of vector using Sequencher 4.0 (Gene Codes Inc., Ann Arbor, MI, USA). Base calls were confirmed both manually and automatically via PHRED (CodonCode Inc., Dedham, MA, USA). SSU rRNA sequence data were compiled and aligned to full-length sequences obtained from GenBank using the FASTALIGNER alignment utility of the ARB program package (www.arb-home.de). Alignments were verified by comparing the secondary structure of the sequences to *Escherichia coli* and closely affiliated phylotypes. Phylogenetic analyses of the bacterial SSU rRNA genes were generated in PAUP* version 4.0b10 (Sinauer Assoc. Inc., Sunderland, MA, USA) using distance and parsimony methods. SSU rRNA sequence distances were estimated using the Kimura two-parameter model, and bootstrapping for distance and parsimony was accomplished with 1000 replicates per tree, using heuristic search methods.

Laboratory fuel cells

Two fuel cells were prepared in the laboratory using only dissolved sodium sulfide as an electron donor. The first was assembled from two identical 1.5-L custom-made glass chambers with side arms (Ace Glass, Vineland, NJ, USA), an o-ring joint that sealed against a Nafion–117® cation exchange membrane (Aldrich Chemical Company, Milwaukee, WI, USA), matching anode and cathode (14.5-cm-long by 1.27-cm in diameter G-10 graphite rods, Graphite Engineering Inc.), and filtered (1 μm) and autoclaved seawater as the electrolyte. All glassware, plasticware, and electrodes were autoclaved before use for 20 min at 120 °C. The cathode chamber also contained a bare-wire Ag/AgCl reference electrode.

The anode chamber was stirred continuously with a magnetic stirrer, and after flushing with nitrogen gas, sodium sulfide was added from a 100 mM stock to yield a sulfide concentration of 1 mM. The cathode chamber was open to the atmosphere and continuously aerated. Air and nitrogen gas were passed through separate 0.3 mm-pore-size HEPA-VENT filters (Whatman, Middlesex, UK) prior to entering the fuel cell. The cell voltage was controlled using a Model DLK60 potentiostat (Analytical Instrument Systems Inc., Flemington, NJ, USA), while whole-cell potential, anode potential (vs. Ag/AgCl) and current were recorded by a logging multimeter (Agilent 34970 A data acquisition unit with a 20-channel multiplexer module, 34901 A; Agilent Technologies, Palo Alto, CA, USA).

This simple chemical cell was maintained at open circuit until a nearly steady cell potential was achieved (*c.* 540 mV after about 4 days). Then to allow comparison to the polarizations of FC1 and FC2, the cell voltage was stepped down from 500 to 150 mV in 50 mV steps once each day, after which the potentiostat was disconnected, and the cell allowed to return to a steady open circuit potential. Two days into this open circuit period, the sulfide concentration was adjusted back up to 1 mM based on measurements of the sulfide concentration. When the cell voltage had become stable again (*c.* 650 mV), another polarization was conducted identical to the first, except that it was started at 600 mV.

For the second laboratory fuel cell experiment, a larger two-chamber system was designed to more closely resemble the field cells, and it was used to evaluate the effects of total dissolved sulfide at very high concentrations similar to an ocean seep. Each half-cell was constructed from a 5-L cylindrical flask equipped with a sidearm ending in a 60-mm Schott flange tooled to accept an o-ring (Ace Glass; custom design); the Nafion membrane was pressed against the cathode side with a CAPFE o-ring, and the joint held in place with a quick release clamp. The top of each chamber was equipped with a 150-mm Schott flange, sealed with a silicone o-ring, and each cap was equipped with seven 24/40 ground glass female inlet ports. The anode chamber was fitted with a graphite rod anode (Graphite Engineering and Sales; grade G-10; 14.5-cm long × 1.27 cm in diameter), a pH combination electrode (Microelectrodes Inc., Bedford, NH, USA), and a polyfluoralomer (PFA) tube [Cole Parmer, (Vernon Hills, IL, USA) 1/4″ od] for N_2 bubbling. The cathode side held a 0.5-m-long carbon brush electrode (Kongsberg-Simrad), a Ag/AgCl/3 M KCl reference electrode (Microelectrodes Inc.), a temperature probe [HOBO TMC6-HD connected to a U12-012 Onset Computer (Pocasset, MA, USA) logger], and a PFA tube connected to a glass gas dispersion tube for air bubbling.

All unused ports were closed with ground glass stoppers equipped with Teflon® sleeves (Ace Glass) with the exception of one port on the cathode chamber which was covered loosely with aluminium foil to allow air to escape. With the exception of the 0.7 M NaCl (used instead of seawater to avoid precipitation losses of sulfide), all apparatus and electrodes were sterilized by autoclaving or by rinsing in denatured alcohol. The NaCl solution was prepared from deionized water and unopened containers of NaCl, and the presumed low

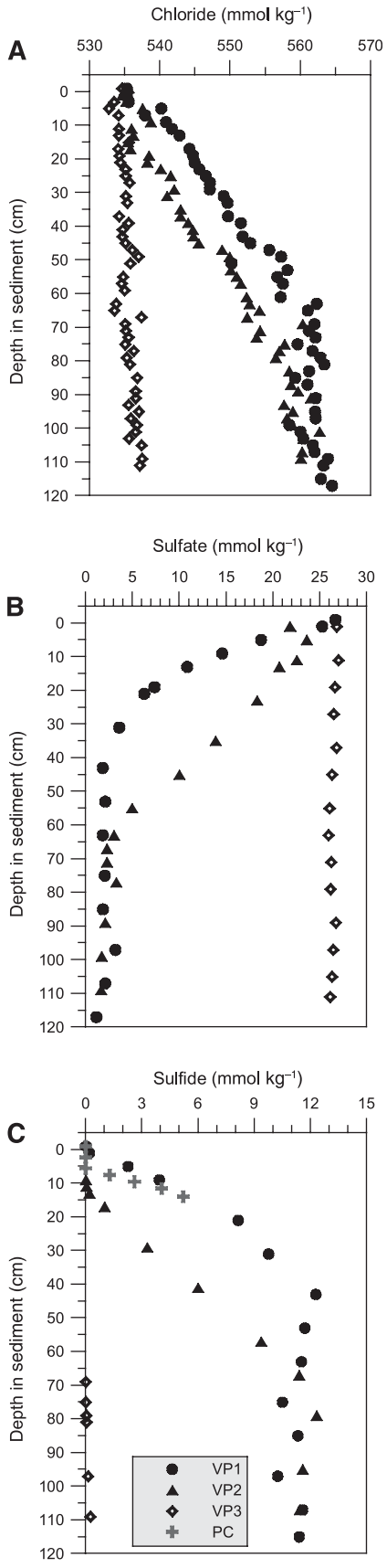

Fig. 3 Pore water distributions of chloride (A), sulfate (B) and total sulfide (C) at Extravert Cliff. Vibrapeeper (VP) profiles were first reported by Plant *et al*. (2001) after *in situ* equilibrations from June 5 to July 11, 2001. Push core 13 was collected on May 21, 2003 immediately next to FC1. VP1, VP2 and PC13 were each positioned within patches of vesicomyid clams. VP3 was positioned in nearby sediments unaffected by seepage.

Table 1 Bottom seawater conditions at Extravert Cliff based on averages of ROV-mounted sensor measurements and laboratory analyses* of Niskin bottle samples taken during BMFC deployment and recovery dives

Temperature (°C)	Salinity	Chloride (mmol kg^{-1})	Dissolved oxygen (μmol kg^{-1})	Dissolved nitrate (μmol kg^{-1})
3.97	34.49	538	14 (18*)	42*

bacterial population, combined with the lack of nutrients and substrate, was judged to render any biological contribution to current insignificant. The contents of both cathode and anode chambers were mixed continuously with magnetic stirrers and purged with nitrogen or air as described above.

After 10 days of initial equilibration, sodium sulfide was added to the anode chamber of this second laboratory cell six times, once every 12 h, from a 1.03-M stock to yield the following sulfide concentrations: 0.3, 1.0, 2.0, 4.0, 8.0 and 12.0 mM. Throughout these procedures both anode and cathode were connected to a passive potentiostat designed and built for these experiments (North-West Metasystems, Inc., Bainbridge Island, WA, USA). This circuit allowed the whole-cell potential to rise to a set voltage (0.3 V), then allowed current to pass to maintain the set voltage.

After each addition of sulfide, the pH within the anode chamber rose to between 10.0 and 11.6, and then it was readjusted to between 7.5 and 8.3 by adding 6 M HCl under N_2 flush with a pasteur pipette. This pH adjustment was performed to simulate more closely pore water chemical conditions. After the final sulfide and HCl addition, voltage and current were monitored for 51 days during which time the sulfide concentration was measured periodically. After 27 and 48 days, the sulfide concentration was readjusted to *c.* 12 mM to replace the losses to oxidation. In both laboratory experiments, determinations of total dissolved sulfide followed procedures adapted from Cline (1969).

RESULTS

Pore fluid chemistry and BMFC performance days 1–26

At Extravert Cliff, seep fluids come to the surface in areas with very small horizontal extent, but are highly altered relative to the bottom seawater (Figs 2 and 3, Table 1). Total sulfide concentrations plateau at about 12 mmol kg^{-1} between 0.4 and 1.2 m below the sediment–water interface (below the influence of the vesicomyid clams), and chloride is also enriched. Other chemically reduced solutes include ammonium (>2 mmol kg^{-1}) and methane (>300 μmol kg^{-1}) (Barry *et al.*, 1997). Less than 1 m from the centre of a

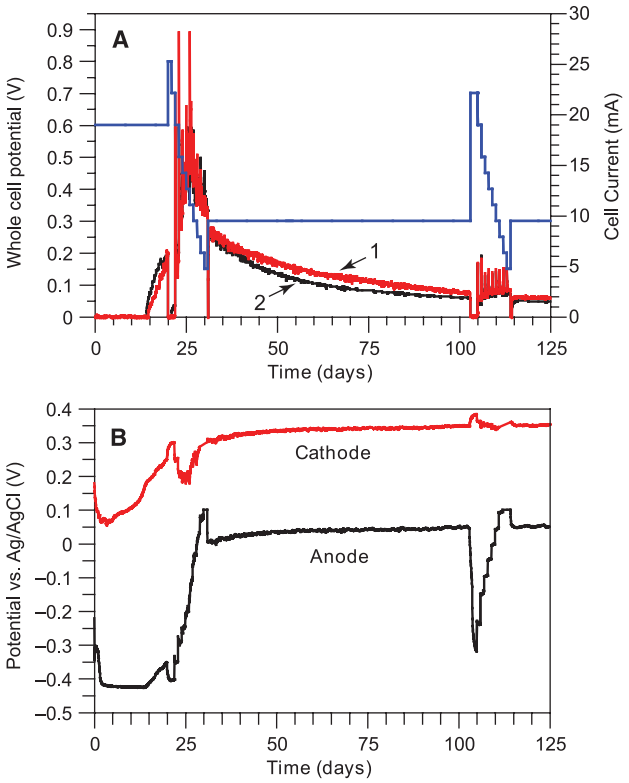

Fig. 4 BMFC performance at a seep in Monterey Canyon. (A) Current production by FC1 and FC2 as a function of programmed cell voltages (shown in blue). (B) Cathode and anode potentials relative to a bare Ag/AgCl reference exposed to bottom seawater during FC2; rising anode potentials at days 20–31 and 103–114 are due to polarizations P1 and P2, respectively.

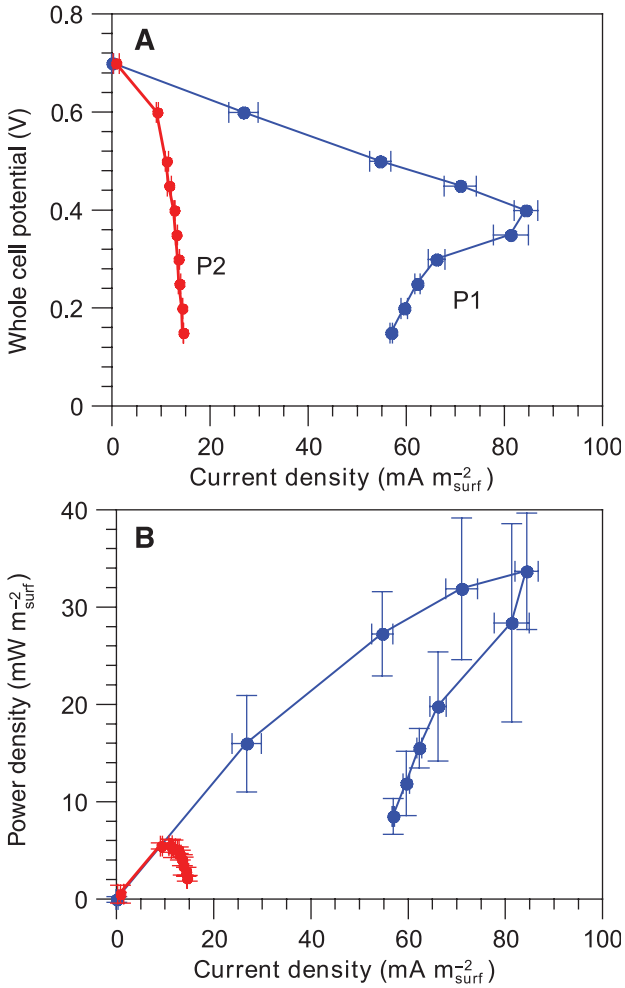

Fig. 5 Polarization effects. (A) Current densities from FC1 as controlled by cell potential. Current density measurements are given relative to the surface area of the graphite anode. Hourly recordings taken between 12 and 24 h after daily downshifts in whole cell potential were averaged to represent quasi-steady state values during experimental days 20–31 (P1) and 103–114 (P2). The error bars reflect 1 SD from the mean. (B) Same results presented as power densities.

seepage site, pore fluids have background concentrations of most constituents (Fig. 3).[1]

On inserting the inert graphite anodes in the sediments of the seepage sites, anode potentials dropped within 3 days to −0.420 V vs. Ag/AgCl (in seawater), equivalent to a measured E_h = −0.184 V. These values did not change appreciably with time until cathode potentials rose high enough for the cells to produce current at the initially set discharge potential of 0.6 V (Fig. 4). Anode potentials shifted much more than cathode potentials once a full cathode potential had developed. We have observed that after new carbon fibre or solid graphite electrodes are first put in seawater, cathode potentials will rise sigmoidally over 6–25 days with or without current flow, and in raw but not sterile seawater systems. In this experiment, the same behaviour occurred. The maximum cathode potential was 0.384 V vs. Ag/AgCl (day 105) indicating a bottom water E_h value of 0.620 V. The minimum anode potential was −0.427 vs. Ag/AgCl (day 11). Both of these extremes in potential were observed at times of zero current.

Cell currents when observed were a function of cathode state, preset whole cell voltage and duration of discharge. The greatest currents were observed during the first polarization (days 20–31; Fig. 4A). These results, especially when viewed as polarization curves (Jones, 1996) (Fig. 5A), indicate that some anode process became limiting when the whole cell voltages were <0.4 V (experimental day 26 and beyond). Maximum sustained (24 h) power levels during the first polarization experiment occurred at a potential difference equal to 0.4 V, averaging 34 mW m^{-2} of anode outer surface area (Fig. 5B). If equated to the footprint area of this anode configuration, the maximum sustained power density was 1100 mW m^{-2} of seafloor.

BMFC performance days 27–125

By the end of the first polarization, the cumulative charge passed by FC1 and FC2 was 11 100 and 11 900 C,

[1] More data from vibrapeepers and push cores are available upon request from Clare Reimers (OSU) or Geoff Wheat (MBARI).

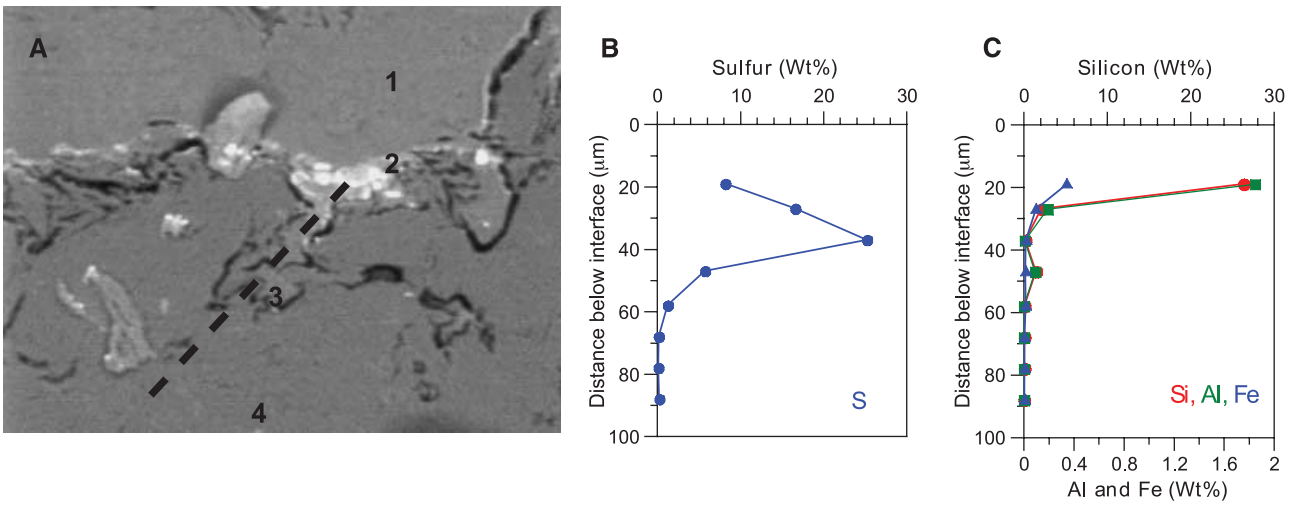

Fig. 6 Surface analyses from the MIDDLE region of the FC2 anode. (A) Electron backscatter image showing a polished cross-section of the outer surface of the anode. Area 1 is epoxy. Area 2 marks a biofilm and entrapped mineral grains. Area 3 is a pore within the graphite. Area 4 is solid graphite. The dashed transect line (70 µm long) corresponds to the locations of points of analysis by electron microprobe. (B) The distribution of sulfur along the dashed transect. (C) Distributions of Si, Al and Fe along the dashed transect.

respectively. In terms of cumulative electron flux, these numbers equate to 0.63 and 0.67 mol m^{-2} anode surface area. Over the next 72 days while held at a whole cell potential of 0.3 V, both fuel cells exhibited slow and steadily declining current. By the second polarization, maximum sustained power levels were less than 6 mW m^{-2} (Fig. 5B), and these levels continued to decline during the second continuous discharge at 0.3 V (days 115–125). The cumulative charge passed by the time of the last recording on day 125 was 41 900 and 37 100 C for FC1 and FC2, respectively. These values represent cumulative electron fluxes to the anode of 2.4 and 2.1 mol m^{-2}.

Anode alterations

When recovered on board ship, the FC2 anode was coated with a biofilm that gave the graphite a glistening appearance. Microprobe analyses of the cross sections of the biofilm and underlying graphite from three depths along the anode indicated widespread but uneven sulfur deposition at the graphite interface and within pores connected to the interface (Fig. 6). The highest sulfur concentrations were observed in subsurface pores, but there were no marked differences between samples cut from different sections of anode. The biofilm (2–35 µm thick) contained trapped mineral grains especially within recessed areas and exhibited elevated Si, Al and Fe concentrations that were not detected in the pores (Figs 6 and 7).

Microbial community analysis

To insure thorough representation of microbial diversity and to provide a crude proxy of abundance, we sequenced and compared 960 plasmids containing rRNA fragments representing phylotypes recovered from the electrodes. The resulting bacterial clone libraries yielded representative phylotypes from the β-, γ-, δ-, and ε-proteobacteria, as well as other groups (Fig. 8). The diversity of bacterial rRNA genes increased with anode depth (i.e. the TOP anode section was least diverse, while the BOTTOM anode section was most diverse). The clone library constructed from the TOP of anode was dominated by SSU rRNA genes from *Desulfuromonas*-like phylotypes (approximately 90%, *c.* 346 clones; Fig. 8), phylogenetically similar to anode communities in previous studies where the electrodes were not deeply buried (Holmes *et al.*, 2004b). Other phylotypes were also recovered from the TOP section, e.g. *Thiothrix* and an uncultivated hydrocarbon seep bacterium (Fig. 8). The MIDDLE clone library was more diverse, with nearly comparable representation of ε-proteobacteria, *Desulfocapsa* and *Desulfuromonas* phylotypes (23, 19, and 16%, respectively; Fig. 8). Dominant representative SSU rRNA genes in the BOTTOM clone library were related to ε-proteobacteria and *Syntrophus* δ-proteobacteria (32% and 24%, respectively; Fig. 8). However, the BOTTOM library also contained numerous phylotypes of the Candidate Division OP1 and OP11 phylotypes, who together represent nearly 25% of the sequenced genes (Fig. 8). In addition, two sequences were recovered from the BOTTOM library that were related to two species of *Cytophaga* (Fig. 8).

Phylotypes recovered from CATHODE library were phylogenetically distinct from those found on the anode, presumably reflecting the electrochemical differences between these habitats, e.g. the presence of oxygen. The CATHODE library was dominated by genes from *Pseudomonas flourescens*-like phylotypes (49% of *c.* 160 clones; Fig. 8). Genes from phylotypes related to *Janthinobacterium lividum* and

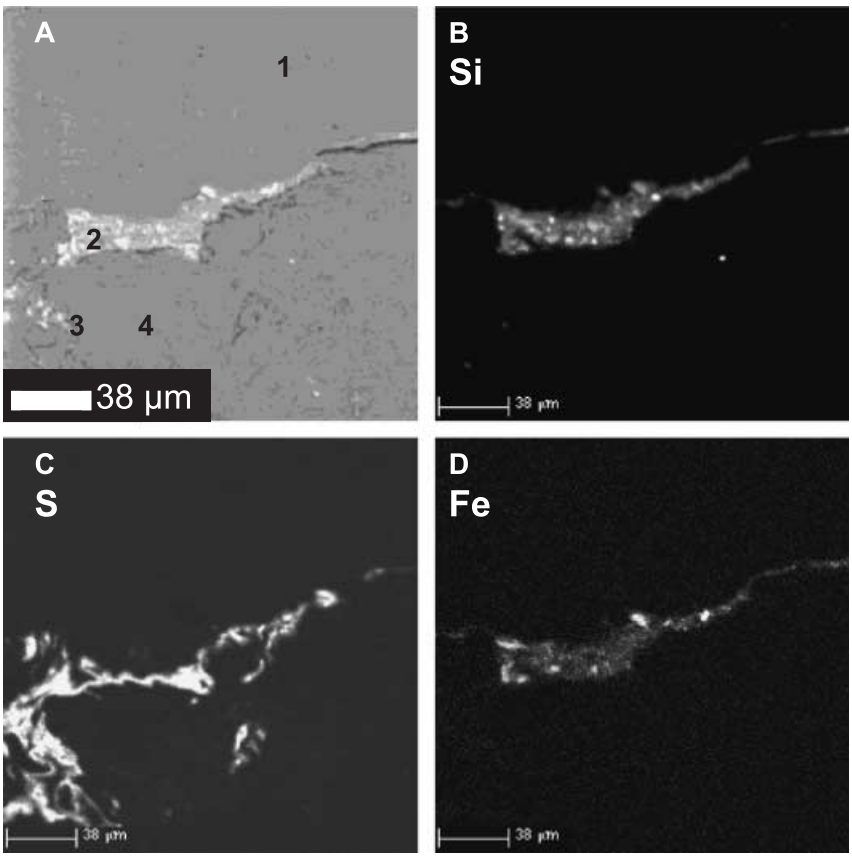

Fig. 7 X-ray spatial patterns of the elements Si (B), S (C) and Fe (D) through a cross-section of the BOTTOM section of the anode surface shown as an electron backscatter image in (A). White areas indicate regions of high concentration relatively. Numbered areas in (a) correspond to the same features identified in Fig. 6.

Aeromonas encheleia constituted 27% and 7% of the CATHODE library, respectively (Fig. 8).

Laboratory polarizations

The build-up of sulfur deposits on the outer surface of the FC2 anode caused us to evaluate directly the impacts of sulfide oxidation on cell performance in the laboratory. In the first experiment using a two-chamber cell and a stirred seawater solution of approximately 1 mM ΣS^{2-} in the anode chamber, repeated polarizations showed no significant change in performance or evidence for concentration polarization[2] (Fig. 9A). The maximum current densities were also less than those observed during the first field polarization and were calculated in the same way (see captions of Figs 5 and 9).

The cumulative electron flux to the anode at the end of this 34-day experiment was 0.225 mol m^{-2} (Fig. 9B) which is roughly equivalent to the cumulative electron flux to the seep anodes at day 24 of the field experiments, or ~10% of the final cumulative flux to the seep anodes at day 125. Dissolved sulfide concentrations decreased between Na_2S additions.

[2] When the concentration of reductant is reduced to zero by reaction at an electrode surface so that the current becomes limited by the rate of mass transfer, an electrode is said to exhibit *concentration polarization* (Bard & Faulkner, 2001).

The second two-chamber laboratory experiment was physically more analogous to the BMFC experiments because a carbon-brush cathode and cylindrical anode were used. Sulfide concentrations were also increased incrementally to the levels observed in seep fluids. The cumulative electron flux to the anode at the end of this experiment was 2.13 mol m^{-2}, very similar to levels achieved in the field. A plot of current density vs. cumulative electron flux (Fig. 10) reveals current density declined as a function of current passed in both the laboratory cell and the field cells. However, only the stirred laboratory-cell current density finally stabilized at approximately 33 mA m^{-2}, and this corresponded to conditions where sulfide concentrations were maintained at concentrations greater than 10 mM. Additions of sulfide to the laboratory cell also generated current spikes that were influenced in large part by pH adjustments. For example, we observed an abrupt 30% drop in current when pH was lowered from 11.60 to 8.35 at a total sulfide concentration of 8 mM. Daily temperature variations in the laboratory also produced fluctuations in the current density of the laboratory cells on the order of 1.3 mA m^{-2} per °C.

DISCUSSION

In this study, BMFCs with graphite anodes having geometric surface areas of 0.184 m^2 and carbon-brush cathodes

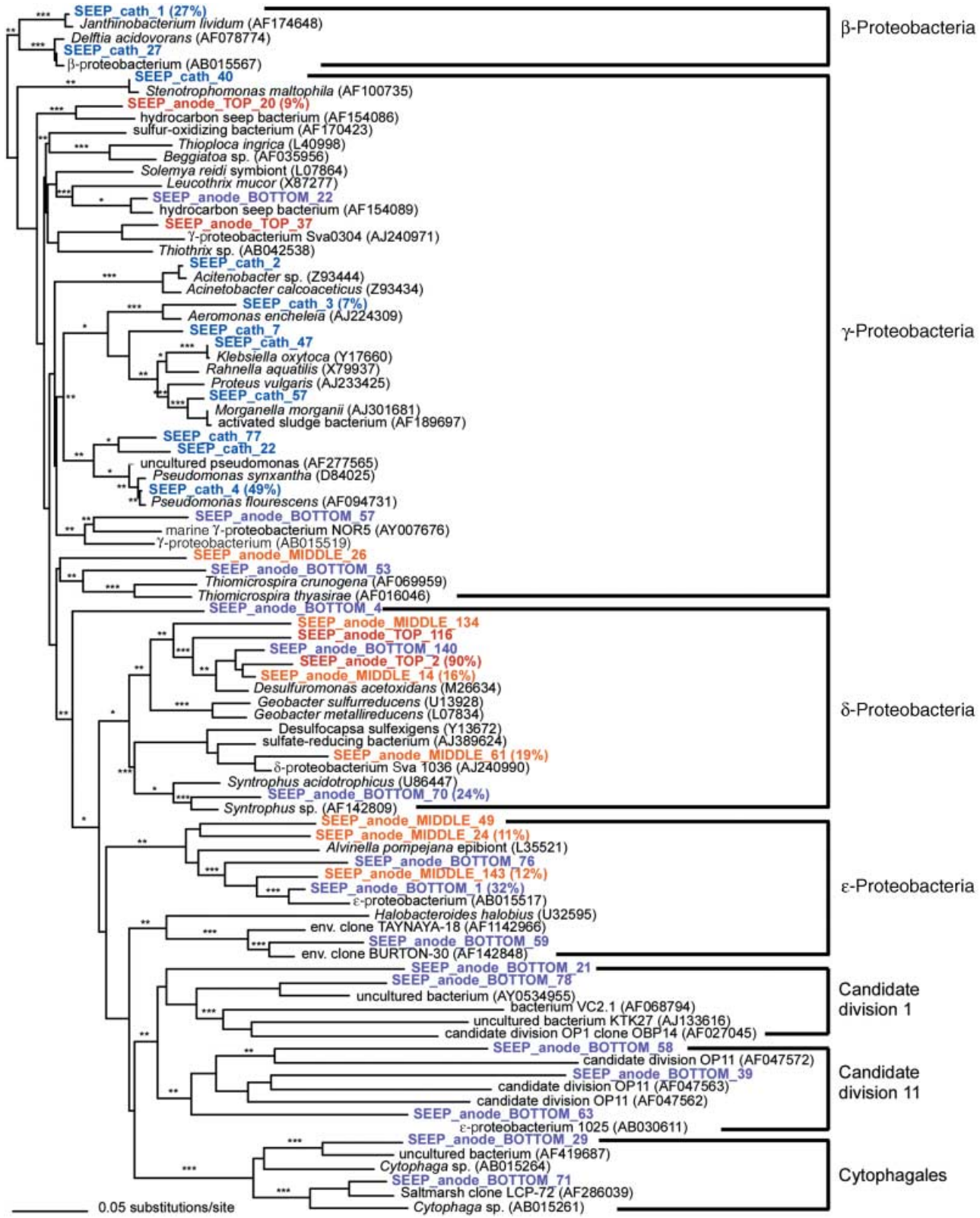

Fig. 8 Phylogenetic tree showing dominant bacterial phylotypes from the anode and cathode of a BMFC deployed in a seep in Monterey Canyon, CA. The three most dominant phylotypes from the cathode or anode section are noted by their percent representation in the clone library. Sequences recovered from the cathode = SEEP_CATH; top of anode = SEEP_anode_TOP, middle of anode = SEEP_anode_MIDDLE, and bottom of anode = SEEP_anode_BOTTOM. (Bootstrap percentages of are indicated as follows: 50–75% = *, 75–99% = **, 100% = ***).

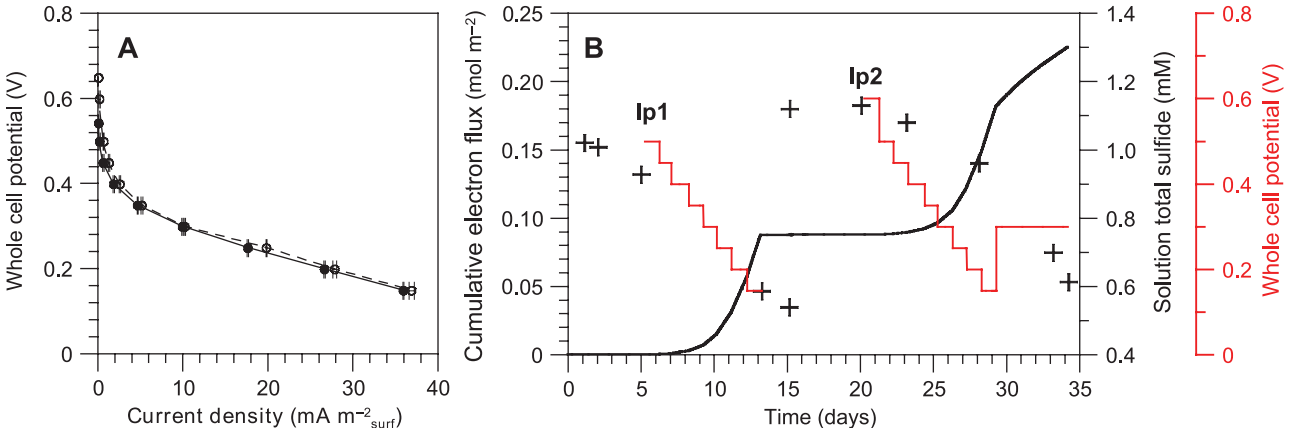

Fig. 9 Two laboratory polarizations run in sequence in an anoxic solution of sterile seawater spiked with Na_2S at time = 0 and 15.13 days. Current measurements were made every 10 min and whole cell potentials were left at open circuit or set to fixed values as shown by the red traces in (B). To compute the current densities, currents measured between 12 and 24 h after daily downshifts in whole cell potential were averaged to represent quasi-steady state values during experimental days 5.2–13.2 (Ip1; closed symbols in A) and 20.3–29.3 (Ip2; open symbols in A). The cumulative electron flux to the anode due to the oxidation of sulfide in shown in (B) as a solid black trace.

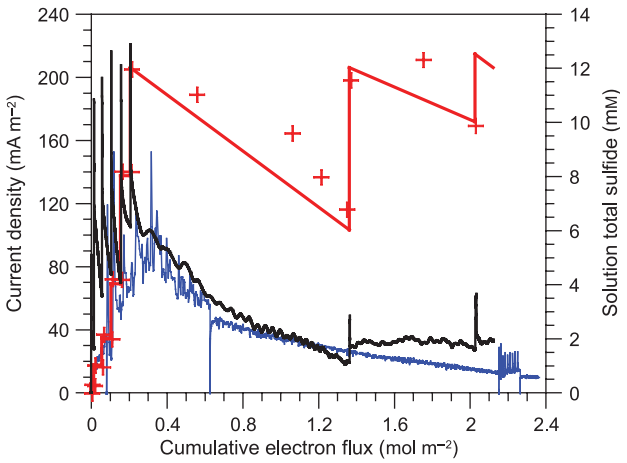

Fig. 10 Current densities as a function of the cumulative electron flux to the anodes of FC1 (blue trace) and a laboratory fuel cell bathed in 0.7 M NaCl spiked with Na_2S and HCl (black trace). Sulfide concentrations (right axis) measured on discrete samples withdrawn from the laboratory anode chamber are shown by the red crosses overlain with nominal sulfide concentrations calculated based on Na_2S additions (red trace). Current density spikes appear immediately after sulfide additions to the laboratory cell.

demonstrated a maximal sustained (24 h) power density of 34 mW·m^{-2} equating to 1100 mW m^{-2} of seafloor. Although modest, these power levels result from the first demonstration of a BMFC in the deep ocean, and they are approximately three times higher than power densities obtained with similar electrode materials in coastal sediments (Ryckelynck *et al.*, 2005).

Not surprisingly, the factors and processes that dictated the performance of the BMFCs at a cold seep were found to be complex. Over most of the experiment, cathodic potentials did not fall below 330 mV vs. Ag/AgCl, but anodic potentials rose by more than 400 mV (Fig. 4B). This indicates anodic rather than cathodic processes were limiting over the long-term, even though bottom-water oxygen concentrations were low at the seep site (Table 1) and the cathode fibers of the carbon-brush electrodes became surrounded by a thick biofilm. Seawater biofilms have been found to have remarkably efficient catalytic properties for oxygen reduction in previous studies (Bergel *et al.*, 2005). In this field demonstration, the equilibrium cathodic potential (0.384 V vs. Ag/AgCl) and dominance of *P. fluorescens* within the cathode clone libraries is highly suggestive that manganese oxides and oxyhydroxides (Rhoads *et al.*, 2005) and/or phenozines (Hernandez & Newman, 2001) played a major role in maintaining activity of the cathode in a low-oxygen environment.

Our molecular phylogenetic analyses of microbial biofilms that formed on the anode surface revealed changes in microbial community composition along the anode as a function of sediment depth. Within the 20–29 cm sediment horizon, the anodic biofilm was dominated by micro-organisms phylogenetically allied to *Desulfuromonas acetoxidans*. We suspect the availability of Fe(III) in the surrounding sediments or other geochemical factors, restricted their distribution and abundance so as to enrich only the TOP section of the anode. *D. acetoxidans* is capable of supporting growth by oxidizing organic compounds, such as acetate, and transferring these electrons to electrodes (Holmes *et al.*, 2004a). Phylotypes within the *Geobacteraceae*, like *D. acetoxidans*, have also been shown to transfer electrons to Fe(III) oxides via a membrane-bound Fe(III) reductase (Nevin & Lovley, 2000; Magnuson *et al.*, 2001; Childers *et al.*, 2002). These results support prior observations that, where they are present in the surrounding sediment, there will be a specific enrichment of micro-organisms capable of Fe(III) reduction on the anodes of BMFCs (Holmes *et al.*, 2004b).

The MIDDLE (46–55 cm depth) and BOTTOM (70–76 cm depth) sediment horizons enriched for other, more diverse, communities on the anodic surface, with SSU rRNA genes from *Geobacter*-like phylotypes representing approximately 16% of 576 sequenced SSU rRNA gene fragments (Fig. 8). In the MIDDLE sediment horizon, phylotypes from both the ∂- and ε-proteobacteria, including phylotypes allied to *Desulfocapsa*, were nearly equally represented in the clone libraries, whereas the BOTTOM horizon was dominated by phylotypes allied to *Syntrophus acidotrophicus*, the ε-proteobacteria, and Candidate Division OP1 and OP11 (Fig. 8). *Desulfocapsa* are sulfate-reducing bacteria known to derive energy for growth from the disproportionation of S^0 (Finster *et al.*, 1998). Their abundance on the FC2 anode at this horizon, is likely linked to the sulfur deposits observed on the surface (see following discussion), and prior studies have suggested that they may help remove those deposits by regenerating sulfate and sulfide (Ryckelynck *et al.*, 2005). *Syntrophus acidotrophicus* is a recently described anaerobic bacterium that, in culture, degrades fatty acids and benzoate in syntrophic association with hydrogen-utilizing micro-organisms (Jackson *et al.*, 1999). In contrast, it is difficult to infer the function of the dominant ε-proteobacteria or phylotypes from Candidate Division OP1 and OP11, as both were most closely allied to uncultivated phylotypes. Related ε-phylotypes have been shown to reduce a variety of inorganic compounds including nitrate, nitrite, polysulfide or dimethyl sulfoxide (DMSO) with formate as the electron donor (Vandamme *et al.*, 1991). The metabolic capacity of OP1 and OP11 remains entirely unknown although their ubiquity in marine and terrestrial environments may imply a prominent role in global geochemical cycling (Harris *et al.*, 2004).

Overall, the observed phylogenetic diversity of the anode does not support linking electricity generation to a single electron transport process when considering energy harvesting from aquatic sediments. If we assume that the elongated anodes functioned as a solid-phase terminal electron acceptor at all sediment depths, then it is likely that the phylotypes enriched in the TOP, MIDDLE and BOTTOM horizons are equally capable of either direct or mediated extracellular electron transfer (i.e. electron hopping through mediators within the biofilm). We make this claim, however, with the cautionary acknowledgement that one cannot definitively infer function or activity from phylogeny.

In addition, our laboratory experiments with chemical fuel cells illustrate that reduced substrates such as hydrogen sulfide will certainly diffuse to a BMFC anode, adsorb, transfer electrons and can slowly deactivate the anode surface. This deactivation should limit both abiotic and biotic electron transfer mechanisms and is attributed largely to passivation by the electrocatalytic deposition of elemental sulfur (Ateya & Al-Kharafi, 2002).

$$HS^- = S + H^+ + 2\,e^- \quad E^\circ = -0.065\ \text{V (SHE)} \qquad (1)$$

A decrease in pH towards the anode over time is expected to shift anodic oxidation reactions of sulfide to give elemental sulfur rather than polysulfide, thiosulfate or sulfate (Hamilton & Woods, 1981; Ateya & Al-Kharafi, 2002). The presence of high concentrations of S especially within pores connected to the graphite surface is consistent with a passive S° film, and one that was more developed than in earlier BMFC experiments in less sulfidic environments (Ryckelynck *et al.*, 2005). Current densities also declined at a rate early in the seep experiment that was comparable to our laboratory experiment run with elevated sulfide (Fig. 10).

However, anodic reactions of BMFC should also be viewed as controlled by mass transfer of reductants from the surrounding environment towards the buried graphite surface. These reductants include organic substrates utilized by the biofilm and inorganic electron donors such as sulfide. Although seeps are characterized by advective fluid fluxes, in the Monterey Canyon these advection rates are estimated to be generally slow (10's cm/year) and intermittent (A. LaBonte and K. Brown, pers. comm., 2005) and so may not have enhanced mass transfer significantly compared to molecular diffusion. An indication of the effect of mass transport limitation of the anodic reactions is given by the polarizations (P1 and P2, Fig. 5). A mass transport barrier appears to have been reached at cell potentials less than 0.4 V that caused a fall in cell current densities. This concentration polarization behaviour (Jones, 1996) was not observed with the first laboratory fuel experiment that had a well-stirred Na_2S solution.

Notwithstanding the progressive effects of passivity we can determine if the extended current records are indeed consistent with mass transport limitation of anodic reactions. First, we note that current densities continued to decline as a function of time or cumulative electron flux in the field experiments in contrast to the second laboratory experiment in which current densities eventually leveled out under stirred conditions with elevated sulfide concentrations (Fig. 10). A model approximation based on conditions for radial diffusion to a cylindrical electrode (with surface area $A = 2\pi r_o l$) after a large amplitude potential step (Bard & Faulkner, 2001) is given by:

$$i = \frac{nFAD_oC_o^*}{r_o}\left[\frac{2\exp(-0.05\pi^{0.5}\tau^{0.5})}{\pi^{0.5}\tau^{0.5}} + \frac{1}{\ln(5.2945 + 0.7493\tau^{0.5})}\right] \qquad (2)$$

where $\tau = 4D_ot/r_o^2$, $F = 9.6485 \times 10^4$ C mol^{-1}, C_o^* is the concentration of dissolved reductant surrounding the anode at time zero, and D_o is the effective Fickian transport coefficient governing radial transport of the dissolved reductant to the cylinder interface. If used to describe the current records of FC1 and FC2, the unconstrained parameters in this relationship are C_o^* and D_o; the model also requires that a diffusion layer can be sustained on a scale larger than the electrode diameter. If C_o^* is restricted to a concentration of 12 ± 2 mM

sulfide, to is assumed to be at the start the high current flow on day 22, and it is assumed that according to equation (1) $n = 2$, iterative applications of the model to the current records between days 31 and 103 (when potential was constant at 0.3 V) predict D_o in the seep sediments was equal to between 0.9×10^{-5} and 1.7×10^{-5} cm^2s^{-1} with coefficients of determination ≥ 0.98 for linear regressions of current vs. the bracketed term of equation (2) for both experiments. This range for a mass transport coefficient is equal to 0.79–1.5 times the free solution diffusion coefficient for HS^- in seawater at 4 °C (Boudreau, 1997), the bottom-water temperature at the seep locations (Table 1). Higher effective concentrations of C_o^*, caused for example by localized regeneration of HS^- or contributions of other reactive reductants or biofilm processes, would mean lower predicted values of D_o. Typically, dissolved solutes diffuse through unlithified marine muds with diffusion coefficients that are reduced to only 0.5–0.7 times free solution coefficients because the path followed by solutes is dependent on the sediment porosity and tortuosity (Ullman & Aller, 1982; Boudreau, 1997). Thus, the current-time records from our BMFC experiments are consistent with sulfide oxidation to elemental sulfur as a primary source of current, while they also imply that solutes were supplied at rates at most only slightly faster than molecular diffusion.

CONCLUSION

BMFCs deployed at an ocean cold seep gave rise to diverse biofilm-forming microbial communities indicating a variety of interactions with current-harvesting anodes and cathodes. In addition, the oxidation of hydrogen sulfide enriched in the seep pore fluids contributed to enhanced power densities initially, while over the long-term the deposition of elemental sulfur slowly deactivated the anode surface and reductant fluxes through the sediments became mass transport limited. This result indicates that in order for the BMFC to be developed into a useful, long-term, environmentally fuelled, power source we must address issues of electrode deactivation and mass transfer limitation while assuming enrichments at the electrodes will be variable and controlled by the environment. Strategies for optimization that have been suggested are:

1 Applying a regenerative-potential program to strip off passivating films (Schröder *et al.*, 2003).

2 Running BMFCs with cycles of current harvesting and no current, combined with cycling between spatially separated anodes.

3 Configuring a high-surface area anode within a chamber supplied with pore fluids by vertical advection (at more active seeps).

We believe combinations of these approaches will lead to an efficient BMFC design that can sustain the power requirements of environmental sensors while yielding insights into biogeochemical processes.

ACKNOWLEDGEMENTS

This work was supported by grants from NOAA's Undersea Research Center for the US West Coast and Polar Regions, the National Science Foundation, Oregon Sea Grant, the Defense Advanced Projects Agency, and the Office of Naval Research. The information reported does not necessarily reflect the position or policy of the Government, and no official endorsement should be inferred. We are grateful to the ROV pilots, ship's crew, technicians, and staff of MBARI's Marine Operations for the successful and safe completion of these experiments, and to Josh Plant, Geoff Wheat and Hans Jannasch for permitting us to report their vibrapeeper pore water data. We also thank Yvan Alleau, Joe Jennings and Kate Howell for analytical assistance, and James Barry and Ed DeLong for information about the study site and added dive time.

REFERENCES

Alberte R, Bright HJ, Reimers C, Tender LM (2005) Method and approaches for generating power from voltage gradients at sediment–water interfaces. United States Patent 6,913,854. Filed 20 October 2000, issued 5 July 2005.

Aller RC (1994) The sedimentary Mn cycle in Long Island Sound: its role as intermediate oxidant and the influence of bioturbation, O_2, and C_{org} flux on diagenetic reaction balances. *Journal of Marine Research* **52**, 259–295.

Ateya BG, Al-Kharafi FM (2002) Anodic oxidation of sulphide ions from chloride brines. *Electrochemistry Communications* **4**, 231–238.

Bard AJ, Faulkner LR (2001) *Electrochemical Methods. Fundamentals and Applications*, 2nd edn. John Wiley and Sons, New York.

Barry JP, Kochevar RE, Baxter CH (1997) The influence of pore-water chemistry and physiology on the distribution of vesicomyid clams at cold seeps in Monterey Bay: implications for patterns of chemosynthetic community organization. *Limnology and Oceanography* **42**, 318–328.

Bennetto HP, Stirling JL, Tanaka K, Vega CA (1983) Anodic reactions in microbial fuel cells. *Biotechnology and Bioengineering* **25**, 559–568.

Bergel A, Féron D, Mollica A (2005) Catalysis of oxygen reduction in PEM fuel cell by seawater biofilm. *Electrochemistry Communications* **7**, 900–904.

Bond DR, Holmes DE, Tender LM, Lovley DR (2002) Electrode-reducing microorganisms that harvest energy from marine sediments. *Science* **295**, 483–485.

Bond DR, Lovley DR (2003) Electricity production by *Geobacter sulfurreducens* attached to electrodes. *Applied and Environmental Microbiology* **69**, 1548–1555.

Borowski WS, Paull CK, Ussler W III (1999) Global and local variations of interstitial sulfate gradients in deep-water, continental margin sediments: sensitivity to underlying methane and gas hydrates. *Marne Geology* **159**, 131–154.

Boudreau BP (1997) *Diagenetic Models and Their Implementation*. Springer, Berlin.

Brett CMA, Brett AM (2002) *Electrochemistry Principles, Methods, and Applications*. Oxford Science Publications, Oxford.

Burdige DJ (in press) *Geochemistry of Marine Sediments*. Princeton University Press, Princeton New Jersey.

Childers SE, Ciufo S, Lovley DR (2002) Geobacter metallireducens accesses insoluble Fe(III) oxide by chemotaxis. *Nature* **416**, 767–769.

Cline JD (1969) Spectrophotometric determination of hydrogen sulfide in natural waters. *Limnology and Oceanography* **14**, 454–458.

Embley RW, Eittreim SL, McHugh CH, Normark WR, Rau GH, Hecker B, DeBevoise AE, Greene HG, Ryan WBF, Harrold C, Baxter C (1990) Geological setting of chemosynthetic communities in the Monterey Fan Valley system. *Deep-Sea Research* **37**, 1651–1667.

Finster K, Liesack W, Thamdrup B (1998) Elemental sulfur and thiosulfate disproportionation by *Desulfocapsa sulfoexigens sp. nov.*, a new anaerobic bacterium isolated from marine surface sediment. *Applied and Environmental Microbiology* **64**, 119–125.

Girguis PR, Orphan VJ, Hallam SJ, DeLong EF (2003) Growth and methane oxidation rates of anaerobic methanotrophic archaea in a continuous-flow bioreactor. *Applied and Environmental Microbiology* **69**, 5472–5482.

Hamilton IC, Woods R (1981) An investigation of surface oxidation of pyrite and pyrrhotite by linear potential sweep voltammetry. *Journal of Electroanalytical Chemistry* **118**, 327–343.

Harris JK, Kelley ST, Pace NR (2004) New perspective on uncultured bacterial phylogenetic division OP11. *Applied and Environmental Microbiology* **70**, 845–849.

Hasvold Ø, Henricksen H, Melvr E, Citi G, Johansen BØ, Kjønigsen T, Galetti R (1997) Sea-water battery for subsea control systems. *Journal of Power Sources* **65**, 253–261.

He Z, Minteer SD, Angenent LT (2005) Electricity generation from artifical wastewater using an upflow microbial fuel cell. *Environmental Science and Technology* **39**, 5262–5267.

Hernandez ME, Newman DK (2001) Extracellular electron transfer. *Cellular and Molecular Life Sciences* **58**, 1562–1571.

Holmes DE, Bond DR, Lovley DR (2004a) Electron transfer by *Desulfobulbus propionicus* to Fe(III) and graphite electrodes. *Applied and Environmental Microbiology* **70**, 1234–1237.

Holmes DE, Bond DR, O'Neil RA, Reimers CE, Tender LM, Lovley DR (2004b) Microbial communities associated with electrodes harvesting electricity from a variety of aquatic sediments. *Microbial Ecology* **48**, 178–190.

Ieropoulos IA, Greenman J, Melhuish C, Hart J (2005) Comparative study of three types of microbial fuel cell. *Enzyme and Microbial Technology* **37**, 238–245.

Jackson BE, Bhupathiraju VK, Tanner RS, Woese CR, McInerney MJ (1999) *Syntrophus aciditrophicus* sp. nov., a new anaerobic bacterium that degrades fatty acids and benzoate in syntrophic association with hydrogen-using microorganisms. *Archives of Microbiology* **171**, 107–114.

Jones DA (1996) *Principles and Prevention of Corrosion*, 2nd edn. Prentice Hall, Inc., Upper Saddle River, New Jersey.

Knapp GP, Stalcup MC, Stanley RL (1990) Automated oxygen titration and salinity determination. Technical Report WHOI-90-35. Woods Hole Oceanographic Institution, Woods Hole, Massachusetts 02543, August 1990. 25pp.

Liu H, Cheng S, Logan BE (2005) Power generation in fed-batch microbial fuel cells as a function of ionic strength, temperature, and reactor configuration. *Environmental Science and Technology* **39**, 5488–5493.

Magnuson TS, Isoyama N, Hodges Myerson AL, Davidson G, Maroney MJ, Geesey GG, Lovley DR (2001) Isolation, characterization and gene sequence analysis of a membrane-associated 89 kDa Fe(III) reducing cytochrome *c* from *Geobacter sulfurreducens*. *Biochemical Journal* **359**, 147–152.

Muller-Karger FE, Varela R, Thunell R, Luerssen R, Hu C, Walsh JJ (2005) The importance of continental margins in the global carbon cycle. *Geophysical Research Letters* **32**, L01602.

Nevin KP, Lovley DR (2000) Lack of production of electron shuttling compounds or solubilization of Fe(III) during reduction of insoluble Fe(III) oxide by *Geobacter metallireducens*. *Applied and Environmental Microbiology* **66**, 2248–2251.

Orange DL, Greene HG, Reed D, Martin JB, McHugh CM, Ryan WBF, Maher N, Stakes D, Barry J (1999) Widespread fluid expulsion on a translational continental margin: mud volcanoes, fault zones, headless canyons, and organic-rich substrate in Monterey Bay, California. *Geological Society of America Bulletin* **111**, 992–1009.

Plant JN, Wheat CG, Jannasch H (2001) A peek at fluid flow in Monterey Bay cold seeps using peepers. *EOS Transactions AGU* **82**, Fall Meeting (Suppl.) Abstract OS42A–0468.

Rabaey K, Boon N, Siciano SD, Verhaege M, Verstraete W (2004) Biofuel cells select for microbial consortia that self-mediate electron transfer. *Applied and Environmental Microbiology* **70**, 5373–5382.

Rathburn AE, Pérez ME, Martin J, Day SA, Mahn C, Gieskes J, Ziebis W, Williams D, Bahls A (2003) Relationships between the distribution and stable isotopic composition of living benthic foraminifera and cold methane seep biogeochemistry in Monterey Bay, California. *G*^{3} **4**, 1–28.

Reguera G, McCarthy KD, Mehta T, Nicoll JS, Tuominen MT, Lovley DR (2005) Extracellular electron transfer via microbial nanowires. *Nature* **435**, 1098–1101.

Reimers CE, Tender LM, Fertig SJ, Wang W (2001) Harvesting energy from the marine sediment-water interface. *Environmental Science and Technology* **35**, 192–195.

Rhoads A, Beyenal H, Lewandowski Z (2005) A microbial fuel cell using anaerobic respiration as an anodic reaction and biomineralized manganese as a cathodic reactant. *Environmental Science and Technology* **39**, 4666–4671.

Ryckelynck N, Stecher HA III, Reimers CE (2005) Understanding the anodic mechanism of a seafloor fuel cell: interactions between geochemistry and microbial activity. *Biogeochemistry* **76**, 113–139.

Schröder U, Niessen J, Scholz F (2003) A generation of microbial fuel cells with current outputs boosted by more than one order of magnitude. *Angewandte Chemie International Edition* **42**, 2880–2883.

Tender LM, Reimers CE, Stecher HA, Holmes DE, Bond DR, Lowy DA, Pilobello K, Fertig SJ, Lovley DR (2002) Harnessing microbially generated power on the seafloor. *Nature Biotechnology* **20**, 821–825.

Tryon MD, Brown KM, Torres ME (2002) Fluid and chemical flux in and out of sediments hosting methane hydrate deposits on Hydrate Ridge, OR, II: hydrological processes. *Earth and Planetary Science Letters* **201**, 541–557.

Ullman WJ, Aller RC (1982) Diffusion coefficients in nearshore marine sediments. *Limnology and Oceanography* **27**, 552–556.

Vandamme P, Falsen E, Rossau R, Hoste B, Segers P, Tytgat R, De Ley J (1991) Revision of Campylobacter, Helicobacter, and Wolinella taxonomy: emendation of generic descriptions and proposal of *Arcobacter* gen. nov. *International Journal of Systematic Bacteriology* **41**, 88–103.